JOURNAL OF GEOPHYSICAL RESEARCH, VOL. 92, NO. B9, PAGES 8969–8975, AUGUST 10, 1987

Analysis of Time Series of Glacier Speed: Columbia Glacier, Alaska

ROY A. WALTERS

U.S. Geological Survey, Tacoma, Washington

WILLIAM W. DUNLAP

University of Washington, Seattle

During the summers of 1984 and 1985, laser measurements were made of the distance from a reference location to markers on the surface of the lower reach of Columbia Glacier, Alaska. The data have numerous gaps, mostly because of inclement weather. The laser measurements were corrected for variations in atmospheric temperature and pressure and for the trajectory of the marker. The marker speed was calculated by using a combination of cubic splines and digital filters to arrive at a data set with 1-hour time intervals. The speed varies from 7 to 15 m/d and has three noteworthy components: (1) a low-frequency perturbation in speed with a time scale of days related to increased precipitation, (2) semidiurnal and diurnal variations related to sea tides, and (3) diurnal variations related to glacier surface melt. The low frequency and tidal period variations are separated by low-pass filtering and subtracting the filtered data from the original data. The variations from melt runoff and tides have the same frequency range and are examined using harmonic analysis and multiple regression with the various forcing functions. The high-frequency portion of the ice speed signal is dominated by tidal influences and to a lesser extent by meltwater influences. The low-frequency portion of the signal is dominated by the effects of precipitation.

INTRODUCTION

Columbia Glacier is a large tidewater glacier located in south central Alaska, west of Valdez (Figure 1). The glacier has an area of about 1100 km^2 and extends 65 km along the main branch from the Chugach Mountains to Columbia Bay in Prince William Sound. The glacier is grounded, and a substantial amount of ice in the lower reach lies below sea level. The terminal moraine is partially submerged with a maximum depth of about 22 m below mean lower low water. The glacier has retreated from this moraine such that the terminus rests in about 200 m of water. The depth increases upglacier to more than 350 m below mean sea level [*Brown et al.*, 1986]. *Post* [1975] surmised that an irreversible retreat would occur if the glacier terminus retreated off the terminal moraine into deeper water. A major research program was begun in 1974 [*Meier et al.*, 1978]. Since 1978, the glacier has retreated 2 km from the terminal moraine.

Recent glaciological research has indicated a need for the better understanding of the relation between ice flow and subglacial water flow [*Kamb et al.*, 1985] and calving rates. As a result, an intensive field program in August and September 1984 collected data on ice calving, ice velocity, terminus position, meteorological variables, tide stage, and runoff from a marginal river (as a surrogate for subglacial discharge). This program is described in detail by *Vaughn et al.* [1985]. The purpose of this report is to analyze the ice speed data and relate its variations with variations in the various forcing functions. The primary focus is the ice speed derived from electronic distance meter (EDM) measurements (EDM, Figure 1); temperature, insolation, and precipitation from meteorological measurements (MET, Figure 1); tide stage at Dalli Bay on Heather Island (DB, Figure 1) and Valdez; and river discharge at the eastern lobe of the glacier (GATE, Figure 1).

In 1985 the field program was expanded to three reflectors allowing for a study of amplitude changes and phase lags in ice speed between three points on the lower reach of the glacier.

DATA SET

The basic data set describes distance from the EDM to the reflector as a function of time and contains numerous gaps. Furthermore, the time base changes for some of the records such that Δt, the time increment between data points, is not constant. In general, the time increment was 15 min for the 1984 data and 10 min for the 1985 data. There were shifts in the time base of up to 2 min for the 1984 data and up to 6 min for the 1985 data. Because some analysis methods used here require an uninterrupted data set and a constant Δt, interpolation is required. A method which allows a straightforward estimation of speed (the first derivative of distance with respect to time), and interpolation of missing or misplaced data is the use of cubic splines fitted to the distance data. Because of measurement errors and noise in the data, some form of smoothing is required. Two methods were examined: one, the use of a smoothing spline that uses a least squares fit to the data, and the other, the use of an exact fit spline with a digital filter applied to the speed values. The smoothing spline does not have a particularly steep slope near cutoff, and there was considerable difficulty assessing the amount of attenuation at tidal frequencies. Furthermore, there was some indication of an erratic frequency response. As a result, an exact fitting spline was used with a digital filter mainly due to the ease of controlling the filter slope and cutoff.

Copyright 1987 by the American Geophysical Union.

Paper number 6B6107
0148-0227/87/006B-6107$05.00

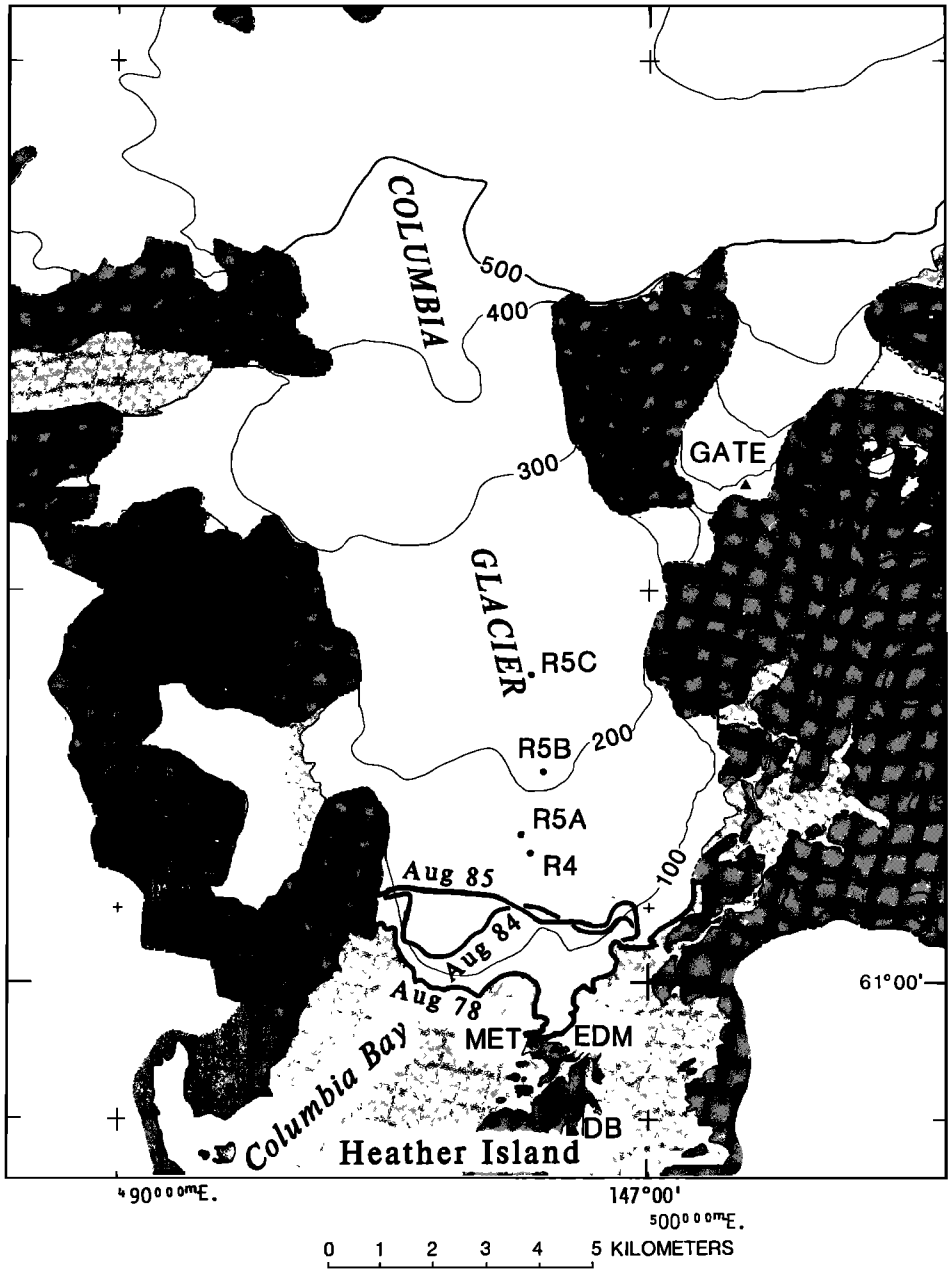

Fig. 1. Index map for Columbia Glacier showing EDM location (EDM), meteorological station (MET), Dalli Bay tide gage (DB), river gage (GATE), and reflectors for 1984 (R4) and 1985 (R5A, R5B, R5C). Surface topography is for August 1978. The contour interval is 100 m (ice) and 200 m (land).

Following the methods described by *Vaughn et al.* [1985], the distance data are adjusted for changes in air density due to changes in temperature and barometric pressure. The data used for this correction were taken at a meteorological station several hundred meters toward the glacier from the EDM (Figure 1, MET). In addition, the ice flow was not along a radius from the EDM, rather at an angle to it. The flow path was fit using a straight line to determine distance along the flow path as a function of time. The speed along the flow path was about 5% greater than the rate of change of distance to the EDM.

Cubic spline interpolation [*Duris*, 1980] was applied to the corrected distance data, and a new time series was interpolated for a constant Δt (15 min for 1984 data and 10 min for 1985 data) and the data gaps were filled. Ice speed values were obtained by differentiating the cubic spline exactly fit to distance along the flow path. A power spectrum for the 1984 ice speed is shown in Figure 2. The spectrum has a rise at low frequency, displays marked diurnal and semidiurnal peaks, and is flat ("white") at higher frequency. The only peak that is significant at the 95% confidence interval is the semidiurnal peak. The high noise levels at high frequency are disappointing because they prevent any analysis of the overtides and nonlinear response of the glacier to the applied forcing. The noise levels in the 1985 speed are larger than the 1984 speed presumably due to the smaller time step (10 min), larger measurement errors from atmospheric inhomogeneities, and larger distances to the markers.

A low-pass filter with a half-power point of 1.6 hours and a cutoff of 1 hour was applied to the ice speed, and the new

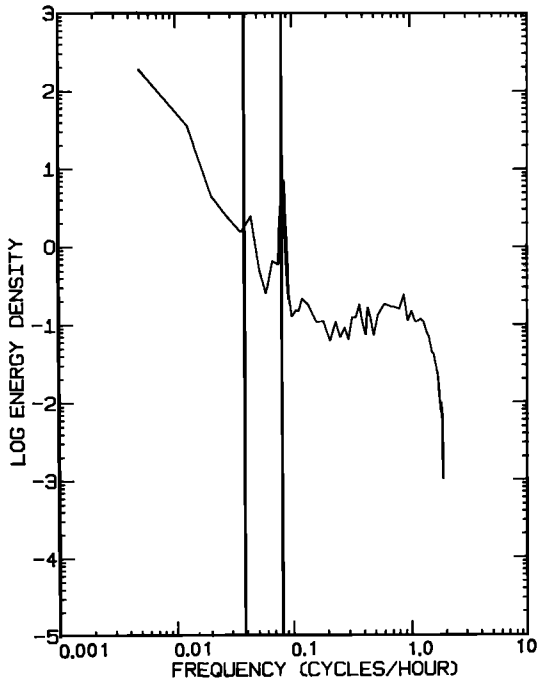

Fig. 2. Power spectra for the 1984 ice speed time series. The vertical lines correspond to the diurnal species K_1 (left) and the semidiurnal species M_2 (right). The flat response from 0.1 to 1 cycle/d indicates the relatively high noise levels in this data.

data set subsampled at hourly values. The filter used is denoted as $A^2{}_nA_{n+1}$, where

$$A_n = \frac{1}{n} \sum_{j=0}^{n-1} S(t + j\Delta t) \tag{1}$$

for a data point at $t + [(n - 1)/2]\ \Delta t$ [see *Godin*, 1972, p. 62] and where S is the speed, t is time, and Δt is the time increment. This filter is robust and suffers few afflictions from ringing or aliasing [see *Walters and Heston*, 1982; *Evans*, 1985]. The resultant ice speed is shown in Figures 3*a* and 4 where $n = 4$ for the 1984 data and $n = 5$ for the 1985 data. Two features are noteworthy. First, there is a large peak in speed at about day 233 of 1984 that is related to a rainstorm; and second, there is a semidiurnal signal with an amplitude of about 1 m/d. These two frequency bands are separated by applying an $A^2{}_{24}A_{25}$ filter to the hourly data to derive the low-frequency portion of the signal (Figure 3*b*). This signal is subtracted from the previous data, leaving the high-frequency portion of the signal (Figure 3*c*) that is used in the harmonic analysis.

The power spectrum described above is useful for exploring various regions of the spectrum for unsuspected oscillations. However, because of its statistical nature and the need for smoothing, few humps and wiggles have statistical significance. Thus the analysis herein leads to harmonic analysis, whose objective is to derive the amplitudes and phases of the major constituents of the signal. For oceanic tides the signal is made up of discrete frequencies primarily clustered about the diurnal and the semidiurnal periods. These frequencies are known and are provided as input information. Here, both the tide and the ice speed are subjected to harmonic analysis to quantify the admittance, i.e., the amplitude ratio and phase between the driving force (tides) and the output (ice speed). The methods used are described by *Foreman* [1977] and by *Godin* [1972]. In general, the ability to separate tidal constituents in the clusters depends upon the total length of record. The usable portions of the speed records allowed at least a 15-day analysis, enabling separation of frequencies that differ by a cycle per lunar month. Data gaps were not included in the analysis. The criterion used to define good data points is that for any given 2-hour interval (±1 hour about the hourly value) there must be at least three observations. The results were not sensitive to whether three or four observations were used as a criterion. Because of the short period of data and the high noise levels, only a few constituents were usable. The results of the analysis for the 1984 and 1985 ice speed, and the corresponding tide at Valdez, are shown in Tables 1 and 2. The largest constituent in the tides is the M_2 (lunar semidiurnal component). This component is sufficiently removed from the diurnal variations in ice melt to offer a good estimate of admittance.

An analysis in the time domain was also examined by using cross correlations between ice speed and the various forcing functions: tide stage, insolation, air temperature, and stream discharge as a surrogate for subglacial flow. The appropriate lags were taken as those that resulted in the highest correlation between ice speed and the input variable, where the lag is defined to be positive when the speed is preceded by the forcing variable. These lags were quite distinct and amounted to 0.7 hour for tide (from harmonic analysis), 8 hours for insolation, and 7 hours for temperature.

The low-frequency portion of the ice speed was examined by using a multiple regression of it against air temperature, insolation, and tide stage. In addition, measurements of discharge at the eastern lobe of the glacier (GATE, Figure 1) were used as a surrogate for subglacial discharge. There is no time series for subglacial discharge because of the difficulty of making such measurements.

RESULTS

The results of the harmonic analysis (Tables 1 and 2) include only the major diurnal and semidiurnal tidal constituents. The analysis is for a 15-day period near the end of the record in 1984 and 1985, as these were the periods relatively free from data gaps. In the nomenclature for the tidal constituents, the subscript denotes the associated species: 1 is the diurnal species at 1 cycle/d and 2 is the semidiurnal species at 2 cycles/d. The letter designates the constituent within each species. For instance, the S_2 is the principal solar component with a period of 12.00 hours, the M_2 is the principal lunar component with a period of 12.42 hours, O_1 is the principal lunar diurnal component with a period of 25.82 hours, and K_1 is the luni-solar diurnal component with a period of 23.93 hours. The latter two correspond to frequencies of 1 cycle per lunar day ±1 cycle per tropical year. The M_2 tidal constituent is the largest species in that it has the best signal-to-noise ratio and is sufficiently separated from the diurnal signals so that it provides the best estimate of admittance.

All the results stated here use the Valdez tide. A detailed analysis of the tide at Dalli Bay and at Valdez indicates that the tide at Dalli Bay leads the tide at Valdez by 4 min, with no attenuation of the diurnal species and about a 3% attenuation of the semidiurnal species. The phase lead corre-

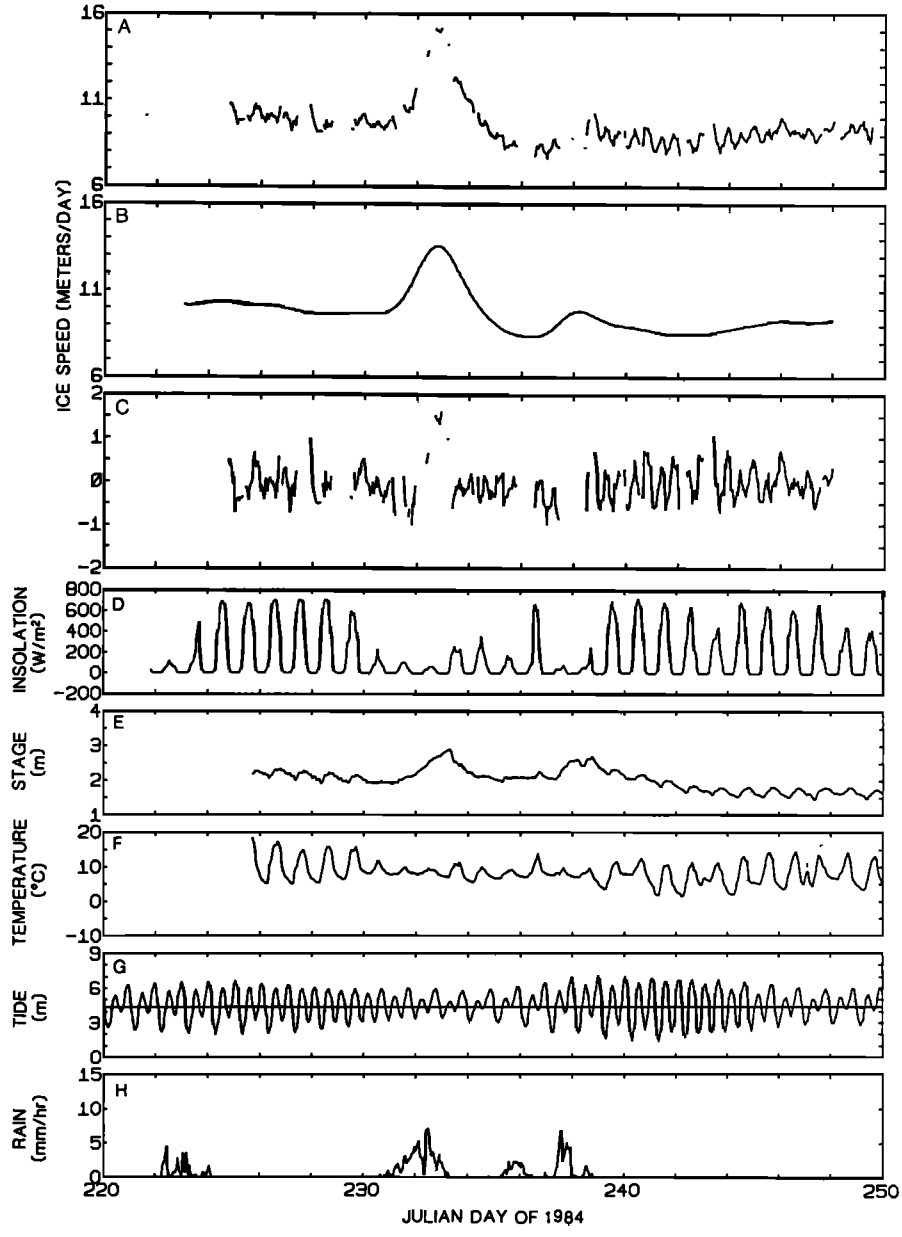

Fig. 3. Graph of ice speed for the 1984 EDM data. (*a*) Speed with gaps filled by cubic spline interpolation and differentiation. (*b*) Low-pass filtered speed with a 24-hour period cutoff. (*c*) The high-frequency portion of the ice speed represented by the difference between Figures 3*a* and 3*b*. (*d*) Insolation at MET. (*e*) River stage at GATE. (*f*) Air temperature at GATE. (*g*) Tide at Valdez. (*h*) Precipitation at MET. Time is in Julian days from January 1, 1984. The tick marks are at 0000 hours.

TABLE 1. Results for the Harmonic Analysis of Ice Speed and Tide (1984)

Species	Frequency, cycles/h	Ice Speed		Tide	
		Amplitude, m/d	Phase, deg	Amplitude, m	Phase, deg
O_1	0.03873065	0.1099	341	0.3200	128
K_1	0.04178075	0.1216	172	0.4756	151
M_2	0.08051140	0.3394	185	1.5240	25
S_2	0.08333333	0.0951	192	0.4845	66

The tide station is at Valdez, Alaska, and lags the tide at Columbia Glacier by 4 min. The analysis period is August 20, 1984, to September 3, 1984.

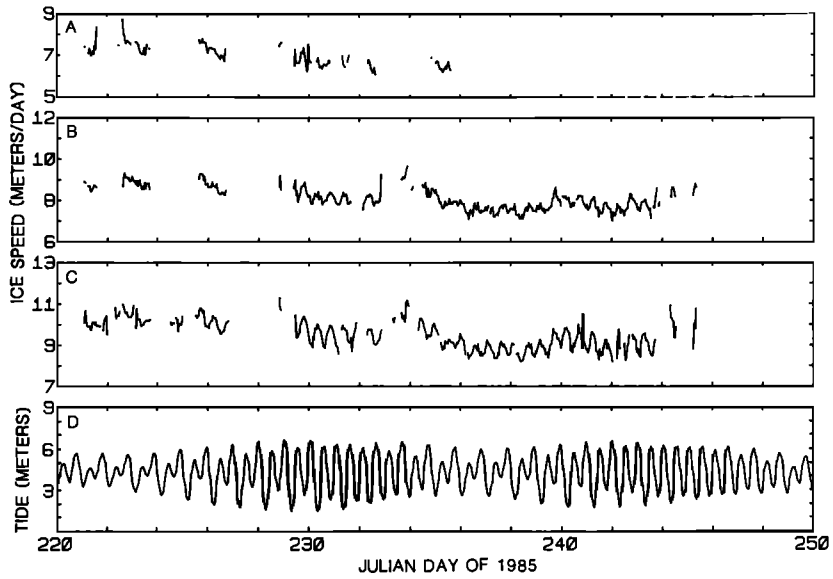

Fig. 4. Graph of ice speed for the three reflectors in 1985. R5A, R5B, and R5C are arranged in an upglacier direction (Figure 1). (*a*) Site R5C. (*b*) Site R5B. (*c*) Site R5A. (*d*) Tide at Valdez.

sponds to about 1° for the diurnal species and 2° for the semidiurnal species. These corrections are so small that the Valdez tide is used directly as a reference because it is a permanent tide station operated by National Ocean Survey and because its record is complete.

The M_2 admittance for the 1984 data has an amplitude of 0.2 m/d for ice speed per meter of tide and a phase of 160°. The latter corresponds to an out-of-phase signal (180°) with a 20° phase lag (−20° or 0.7 hour at the M_2 frequency). The S_2 admittance has similar values (0.2 m/d per m and 130°) although the phase indicates a contamination from the diurnal variation in runoff creating a first harmonic with frequency of the S_2. The criterion used in this assertion is that the frequency response of the system varies smoothly and by a small amount over small frequency ranges; that is, the admittance is smooth [see *Zetler and Munk*, 1975]. Using this criterion, the ice speed variation can be written as a linear combination of dominant forcing functions: tides and surface melt as represented by insolation. That is,

$$\mathbf{S} = r_1\mathbf{h} + r_2\mathbf{I} \tag{2}$$

where **S**, **h** and **I** are vectors in the complex plane defined by their amplitude and phase and represent ice speed, tidal height, and insolation; and r_1 and r_2 are complex-valued admittances also characterized by an amplitude and phase. Writing this equation for both the M_2 and S_2, and solving for r_1 and r_2, the relative effects upon ice speed can be examined. From this analysis, $|r_1| = 0.218$ m/d per m of tide with a phase of 159°, and $|r_2| = 0.000393$ m/d per W/m^2 of insolation with a phase of −91°. At the M_2 frequency, only about 2% of the response in ice speed is nontidal, whereas at the S_2 frequency 22% is nontidal.

Using this criterion on the diurnal species, evidence of effects from other forcing functions is also evident. There is a large difference in the phase response between the O_1 and K_1 constituents. These species are much smaller than the M_2 in the tides, whereas they are a larger component in the diurnal melt. Furthermore, the diurnal melt is characterized by a broad spectral peak rather than a line as in the tides. This is because the diurnal melt fluctuates considerably on a day-to-day basis in response to the weather. For this reason and others the analysis for the diurnal species using (2) is not meaningful. Based upon the O_1 harmonics, the admittance at diurnal frequencies is approximately the same as for the semidiurnal frequencies. The response at the K_1 frequency is heavily contaminated by diurnal melt.

For the 1985 data the admittance has about the same amplitude and phase as the 1984 data for the M_2. The admittance at diurnal frequencies is somewhat different from the values for the 1984 data. These results are consistent with the discussion of the 1984 data, namely, that the best signal is at the M_2 frequency, whereas the diurnal signal is modified by the runoff conditions, which were different in 1985 as shown by the meteorological data.

The results of a harmonic analysis of all three reflectors for 1985 (using the M_2 constituent only) shows that the speed at

TABLE 2. Results for the Harmonic Analysis of Ice Speed and Tide (1985)

		Ice Speed A		Ice Speed B		Tide	
Species	Frequency, cycles/h	Amplitude, m/d	Phase, deg	Amplitude, m/d	Phase, deg	Amplitude, m/d	Phase, deg
O_1	0.03873065	0.0997	243	0.0791	253	0.3123	139
K_1	0.04178075	0.1100	162	0.1588	161	0.4517	154
M_2	0.08051140	0.4457	183	0.2140	189	1.5160	31
S_2	0.08333333	0.1968	219	0.0965	199	0.6037	63

The two reflectors are labeled A and B in an upglacier direction (Figure 1). The tide is measured at Valdez, Alaska. The analysis period is August 17, 1985, to September 1, 1985.

TABLE 3. Results for the Harmonic Analysis of Ice Speed for the Three Reflectors in 1985

Reflector	Distance From EDM, km	Amplitude, m/d	Phase, deg
A	4.0	0.3262	171
B	5.3	0.1989	176
C	7.2	0.0630	172

The analysis period is August 9–23, 1985.

all three points is in phase and its amplitude is reduced markedly in an upglacier direction (Table 3). Note in Figure 4 that there are considerable data missing for the farthest reflector, indicating the difficulty in getting a return at this distance (about 7.2 km) with variable weather conditions. All three data sets were analyzed for the period when the farthest reflector was operating, a period that unfortunately corresponds to the most gaps in the other two data sets. This limits the accuracy of the analysis and hence the results. Within these constraints there was essentially no phase difference between the speed at the three reflectors, of the order of 5° (10 min for M_2) lag. On the other hand, the amplitude decreased in approximately an exponential manner. In many dissipative systems it is common for perturbations at the boundary to dampen exponentially as a function of distance from the boundary. A similar phenomenon is operating in the glacier where the e-folding length (the distance over which the signal decreases to $1/e$) is about 2 km. This length scale seems physically plausible in connection with the work of *Echelmeyer* [1983] at Blue Glacier. He found from observations and numerical model studies that a characteristic length for damping perturbations in this ice flow was approximately 7 times the ice thickness. The ice thickness in the last several kilometers of Columbia Glacier is about 250–350 m, leading to a characteristic length of approximately 2100 m. Thus the observations made at seasonal time scales extend down to semidiurnal time scales, with the caution that this comparison is between different glaciers. Note that this perturbation is a small-amplitude fluctuation that does not significantly alter the mean motion of the glacier. *Meier et al.* [1985] found that velocity fluctuations caused by seasonal changes in the terminus position can be detected up to 8 km above the terminus. There is no contradiction here because the seasonal changes are large amplitude fluctuations that cause a readjustment of the flow field in the lower reach.

Instead of working in the frequency domain, the analysis above can be done in the time domain through the use of regressions between the dependent variable S and the forcing functions h and I. Only tide and insolation are considered here as they lead to the largest reduction in the variance of the residual. The next most important variable was air temperature; however, its inclusion leads to only a 0.4% reduction in the total variance in the ice speed signal when added serially. This contrasts with a 50% reduction for tides and a 17% reduction for insolation. Again, only the high-frequency portion of the signal is considered at this time; the low-frequency portion is considered later.

The appropriate lags used in the analysis are taken to be that lag where the correlation between ice speed and the forcing variable are a maximum. These lags are 1 hour for tide (29° for the M_2), 8 hours for insolation, and 7 hours for air temperature. They are in the sense that ice speed lags behind the forcing variables. The results of the regression are shown in Figure 5 which includes the ice speed for 1984, the predicted speed based upon the regression, the residual between these data, and the forcing functions for tide and insolation. Note that the data are plotted against an index number rather than real time. Hence the data gaps are removed and the data are compressed. The amplitude of the regression coefficient for the tide (0.19 m/d per m of tide) is

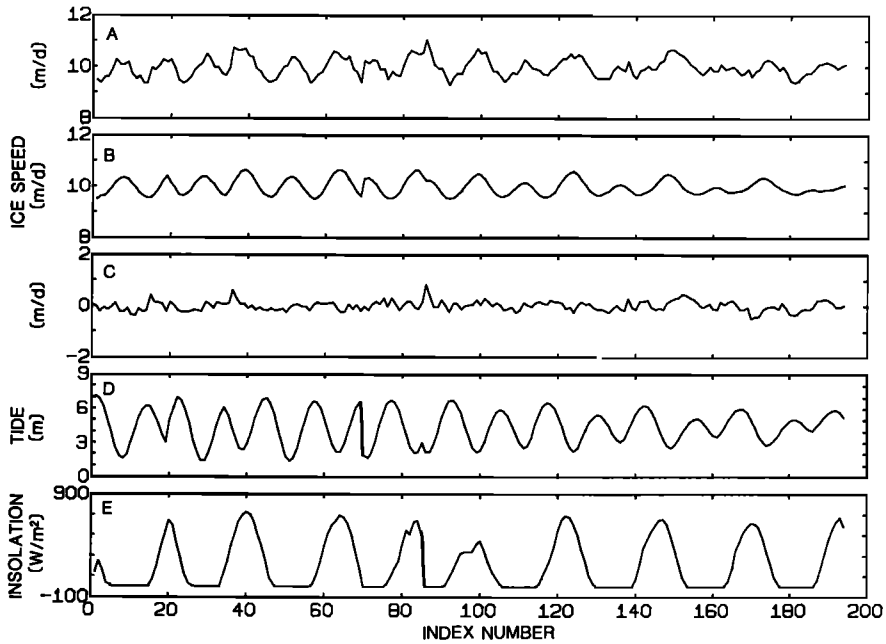

Fig. 5. Results for the multiple regression between ice speed, tide, and insolation (1984). The abscissa is the index number for the data point, not time, because data gaps have been eliminated. (*a*) Ice speed. (*b*) Estimated speed based upon the regression. (*c*) The residual. (*d*) Tide height. (*e*) Insolation. The regression equation is $S = ah + bI$, where $a = -0.19$ m/d per m of tide and $b = 0.00060$ m/d per W/m^2 of insolation.

essentially the same as the amplitude of the admittance calculated earlier. At this point, the regression results could be used to generate the ice speed data in the gaps and replace the data derived from differentiation of the cubic spline.

Next, the low-frequency portion of the ice speed signal (Figure 3*b*) is examined. A thorough analysis is not possible because of the lack of necessary data and the lack of a physical model with which to connect precipitation and speed. However, there are several qualitative features that merit examination. First, ice speed is not a simple function of precipitation. This can be seen by noting the ice speed both before and after the rainstorm around day 233. The ice speed drops approximately 1.3 m/d, which suggests that the drainage system, and hence the basal water pressure, was modified during the precipitation period. Moreover, the second precipitation event around day 238 had a much smaller relative effect upon speed, suggesting that the subglacial drainage was much better developed to accommodate larger discharge. These ideas need to be tested by using deterministic models relating precipitation and basal pressure and relating basal pressure to ice speed [see *Kamb et al.*, 1985].

CONCLUSIONS

The distance data to the reflectors on the glaciers are inherently noisy, and some care must be exercised in processing the data. This analysis uses interpolation based upon cubic splines exactly fitted to the distance data and differentiated to give speed and a digital filter to remove the noise around the sampling frequency.

The high-frequency portion of the ice speed signal (periods of about a day to 0.1 day) was dominated by tidal influences at the terminus. The admittance of the tide was about 0.2 m/d of ice speed per meter of tide height, with a phase of 160° for 1984. Thus the speed fluctuations are out of phase with tide height fluctuations. The tidal period fluctuations in speed were damped in an upglacier direction, decreasing to $1/e$ in about 2 km. There was negligible difference in phase between the three reflectors.

Diurnal variations in glacier melt contributed about one third as much as the tidal contribution to fluctuations in speed. However, these effects were concentrated in the diurnal frequency range as opposed to the semidiurnal range dominated by the tides.

The low-frequency range of the speed (periods of 2 days and longer) was dominated by precipitation effects. However, speed is not a function of precipitation in the sense that a particular amount of precipitation produces a particular value of speed. Rather, speed depends in some measure on the previous state of the system.

Acknowledgments. The authors wish to acknowledge the stimulating discussions with L. A. Rasmussen and M. F. Meier, who also provided helpful reviews of this manuscript. M. F. Meier conceived the EDM project that was carried out by the Glaciology Project in the U.S. Geological Survey.

REFERENCES

Brown, C. S., L. A. Rasmussen, and M. F. Meier, Bed topography inferred from airborne radio-echo sounding of Columbia Glacier, Alaska, *U.S. Geol. Surv. Prof. Pap., 1258-G*, 52 pp., 1986.

Duris, C. S., ALGORITHM 547: Fortran routines for discrete cubic spline interpolation and smoothing [E1], [E3], *ACM Trans. Math. Software*, *6*(1), 92–103, 1980.

Echelmeyer, K. A., Response of Blue Glacier to a perturbation in ice thickness: Theory and observation, Ph.D. dissertation, Calif. Inst. of Technol., Pasadena, 1983.

Evans, J. C., Selection of numerical filtering method: Convolution or transform windowing?, *J. Geophys. Res.*, *90*(C3), 4991–4994, 1985.

Foreman, M. G. G., Manual for tidal heights analysis and prediction, *Pac. Mar. Sci. Rep. 77-10*, 101 pp., Inst. of Ocean Sci., Patricia Bay, Victoria, B.C., 1977.

Godin, G., *The Analysis of Tides*, 264 pp., University of Toronto Press, Toronto, Ont., 1972.

Kamb, B., C. F. Raymond, W. G. Harrison, H. Engelhardt, K. A. Echelmeyer, N. Humphrey, M. M. Brugman, and T. Pfeffer, Glacier surge mechanism: 1982–1983 surge of Variegated Glacier, Alaska, *Science*, *227*(4686), 469–479, 1985.

Meier, M. F., A. Post, C. S. Brown, D. Frank, S. M. Hodge, L. R. Mayo, L. A. Rasmussen, E. A. Senear, W. G. Sikonia, D. C. Trabant, and R. D. Watts, Columbia Glacier progress report—December 1977, *U.S. Geol. Surv. Open File Rep., 78-264*, 78 pp., 1978.

Meier, M. F., L. A. Rasmussen, R. M. Krimmel, R. W. Olsen, and D. Frank, Photogrammetric determination of surface altitude, terminus position, and ice velocity of Columbia Glacier, Alaska, *U.S. Geol. Surv. Prof. Pap., 1258-F*, 41 pp., 1985.

Post, A., Preliminary hydrography and historical terminal changes of Columbia Glacier, Alaska, *U.S. Geol. Surv. Hydrol. Invest. Atlas, 559*, 3 pp., 1975.

Vaughn, B. H., C. F. Raymond, L. A. Rasmussen, D. S. Miller, C. A. Michaelson, M. F. Meier, R. M. Krimmel, A. G. Fountain, W. W. Dunlap, and C. S. Brown, Short-term velocity measurements at Columbia Glacier, Alaska: August–September 1984, *U.S. Geol. Surv. Open File Rep., 85-487*, 29 pp, 1985.

Walters, R. A., and C. Heston, Removing tidal period variations from time-series data using low pass digital filters, *J. Phys. Oceanogr.*, *12*(1), 112–115, 1982.

Zetler, B. D., and W. H. Munk, The optimum wiggliness of tidal admittances, *J. Mar. Res.*, *33*, suppl., 1–13, 1975.

W. W. Dunlap, Statistics, GN-22, University of Washington, Seattle, WA 98195.

R. A. Walters, U.S. Geological Survey, Water Resources Division, 1201 Pacific Avenue, Suite 450, Tacoma, WA 98402.

(Received June 9, 1986;
revised September 12, 1986;
accepted October 15, 1986.)